이학석사 학위논문

Moisture signal on high concentrations of $PM_{2.5}$ in Seoul, Republic of Korea

우리나라 서울에서 $PM_{2.5}$ 고농도에 대한 습도의 영향

2021년 8월

서울대학교 대학원

지구환경과학부

김 가 영

Moisture signal on high concentrations of $PM_{2.5}$ in Seoul, Republic of Korea

우리나라 서울에서 $PM_{2.5}$ 고농도에 대한 습도의 영향

지도 교수 허 창 회

이 논문을 이학석사 학위논문으로 제출함
2021년 4월

서울대학교 대학원
지구환경과학부
김 가 영

김가영의 이학석사 학위논문을 인준함
2021년 6월

위 원 장 김 상 우

부위원장 허 창 회

위 원 장 임 석

Abstract

Moisture signal on high concentrations of $PM_{2.5}$ in Seoul, Republic of Korea

KaYoung Kim
School of Earth and Environmental Sciences
The Graduate School
Seoul National University

The episodes of high concentrations of particulate matter with an aerodynamic diameter less than 2.5 μm ($PM_{2.5}$) were generally occurred under warm and stable high-pressure conditions. The present study found that humid conditions under low-pressure systems play an essential role in the high-$PM_{2.5}$ episodes during the cold seasons (November through March) for 2007-2019 in Seoul, Republic of Korea. The major chemical components of $PM_{2.5}$ were secondary inorganic aerosol species of sulfate, nitrate, and ammonium during the high-$PM_{2.5}$ episodes. The sulfur and nitrogen oxidation ratios, which indicate the magnitude of sulfate and nitrate

formation, increased primarily with relative humidity (RH). Gaseous precursors were actively converted to secondary inorganic aerosols, especially when RH was higher than 60%. These results suggest that the aqueous-phase reaction associated with moisture can accelerate the secondary formation of aerosols, resulting in high-$PM_{2.5}$ episodes. More than half of high-$PM_{2.5}$ episodes occurred under conditions with an RH higher than 60%, and the westward-tilted trough appeared in the lower troposphere. In contrast, high-$PM_{2.5}$ episodes with the RH of less than 60% were associated with photochemical reactions caused by strong insolation in a stagnant high-pressure system. This study suggests that high RH accompanied by low-pressure systems in the lower troposphere can induce high concentrations of $PM_{2.5}$ which should be considered in air quality prediction.

Keyword: $PM_{2.5}$, relative humidity (RH), secondary inorganic aerosol (SIA), aqueous-phase reaction, Seoul

Student Number: 2019-23307

Table of Contents

List of Tables

List of Figures

1. Introduction

Fine particle matter with diameters ≤ 2.5 μm ($PM_{2.5}$) mainly consists of secondary aerosols (Choi et al., 2019; Bae et al., 2020; Kim et al., 2020). In particular, secondary inorganic aerosol (SIA) species of sulfate (SO_4^{2-}), nitrate (NO_3^-), and ammonium (NH_4^+) accounted for more than half of $PM_{2.5}$ in Seoul, the capital of Republic of Korea (Seo et al., 2017; Park et al., 2020). Atmospheric sulfate and nitrate are formed through the oxidations of precursor gases (SO_2 and NO_2) by oxidants (e.g., O_2, OH radicals) via gas-phase, and aqueous-phase reactions (Ravishankara et al., 1997; Zheng et al., 2015). Previous researches have suggested that sulfate in aerosols is usually produced by the homogeneous gas-phase oxidation of SO_2 with subsequent gas-to-particle conversion and aqueous-phase reactions of SO_2 on the liquid particles (Wang et al., 2006; Wang et al., 2016). In contrast, nitrate is mainly formed by the reactions of gaseous HNO_3 or the heterogeneous hydrolysis of N_2O_5 on the aerosol surface (Smith et al., 1995; Adams et al., 1999; Alexander et al., 2009).

Secondary aerosol formations are closely related to meteorological conditions (Jang et al., 2017; You et al., 2017; Ning et al., 2018). A warm and stable ambient atmosphere facilitates the

formation and accumulation of secondary aerosols, resulting in air pollution (Shu et al., 2017; Wai and Tanner, 2005; Zhao et al., 2018). For example, the high concentrations of particulate matter in Seoul occur mainly under high-pressure systems over the Korean Peninsula (Lee et al., 2011; Oh et al., 2015). The stagnant high-pressure system could provide a favorable environment for the accumulation of primary pollutants and secondary aerosol precursors. Furthermore, secondary aerosol production can be activated by high temperature coincident with a large amount of solar radiation under high-pressure conditions. Generally, atmospheric sulfate and nitrate are more likely generated via gas-phase chemistry than aqueous-phase chemistry under high temperatures and solar radiation conditions (Kim et al., 2007; Wang et al., 2016).

Relative humidity (RH) is another important factor in secondary aerosol formation (Quan et al., 2015; Zhao et al., 2013; Tang et al., 2017). The aqueous-phase reaction under humid conditions accelerates the particle conversion of gaseous precursors. Several studies of urban haze events reported that the fractions of SIAs in $PM_{2.5}$ have positive correlations with RH, indicating aqueous chemical processes play important roles in secondary transformation (Guo et al., 2018; Liu et al., 2017; Wu et al., 2018). However, the influence

of RH on the secondary formation of $PM_{2.5}$ has not been clearly identified in Seoul because most of the studies were conducted on short-term cases (Park et al., 2013; Seo et al., 2017). Furthermore, a composite analysis for high-$PM_{2.5}$ episodes in Seoul shows humid conditions in the lower troposphere, but the role of geopotential height and wind fields has been relatively emphasized (Hur et al., 2016; Jung et al., 2019).

This study investigates the influence of relative humidity on $PM_{2.5}$ and the associated synoptic conditions in the high-$PM_{2.5}$ episodes. First, we investigated the characteristics of high-$PM_{2.5}$ episodes in Seoul during the cold season (November through March) in 2007-2019. Secondly, the role of relative humidity in the formation of secondary inorganic aerosols in the high-$PM_{2.5}$ episodes was examined. Finally, the characteristics of the High-$PM_{2.5}$ episodes in wet and dry conditions were compared, including their chemical properties and large-scale atmospheric conditions. A summary is shown in the conclusion section.

2. Data and Methods

2.1 Data

Hourly mass concentration of $PM_{2.5}$ data during the cold seasons (November through March) for 2007–2019 were obtained from 25 air quality monitoring sites in Seoul. The $PM_{2.5}$ concentration data was measured by the beta-ray absorption method after separating each particle less than 2.5 μm from the total particles using an impactor method (Shin et al., 2011; Park et al., 2012). The bias in this method is known to be 10%, mainly due to particle-containing moisture (Chang and Tsai, 2003; Jung et al., 2007). The hourly concentration data is used to obtain the daily average values.

The ion concentrations of $PM_{2.5}$ were obtained from the Seoul Intensive Air Quality Monitoring station from 2012 to 2018. The Seoul Intensive Air Quality Monitoring station is operated to evaluate the impact of local emission sources and to identify the characteristics and causes of high-concentration air pollution cases occurring in urban areas. The ion concentration of $PM_{2.5}$ was measured as BAM-1020 Continuous Particulate Monitor (Met One). The ion component analyzer investigates the concentration of ionic components (SO_4^{2-}, NO_3^-, NH_4^+, K^+, Ca^{2+}, Mg^{2+}, Na^+, and Cl^-). Their measurement methods and accuracy evaluation results of the

concentrations are described in detail in the "2018 Intensive Air Quality Monitoring station Annual Operation Result Report" (NIER, 2018) published by the National Institute of Environmental Research (http://www.airkorea.or.kr). The daily concentrations of CO, SO_2, NO_2, and O_3, which are gaseous reference substances of air pollution, were also produced by the Seoul Intensive Air Quality Monitoring station.

The daily meteorological data of surface air temperature, relative humidity, sea-level pressure, wind speed, surface solar radiation, total cloud cover, and cloud bottom height observed at the Seoul weather station (SWS) for the 2007–2019 cold seasons were acquired from the KMA data portal site. The SWS is the sole synoptic station representing meteorological conditions in Seoul (Ghim et al., 2001). To investigate large-scale atmospheric conditions, daily meteorological variables including geopotential height, relative humidity, and temperature at 500, 850, 1000 hPa levels were analyzed using the ECMWF Reanalysis-5 (ERA5) project reanalysis data. The horizontal resolution of ERA5 is 1.5° both in longitude and latitude.

2.2 Methods

2.2.1 Ambient $PM_{2.5}$ concentration

High-$PM_{2.5}$ episodes are defined using the daily-mean $PM_{2.5}$ threshold value of 35 $\mu g\ m^{-3}$ based on the criteria for $PM_{2.5}$ concentration specified in the environmental protection law of the Republic of Korea. To distinguish the high-$PM_{2.5}$ episodes caused by the anthropogenic sources from those caused by natural sources such as Asian dust storms, yellow dust days announced by the Korea Meteorological Administration were excluded from this analysis.

2.2.2 Oxidation ratio of secondary inorganic aerosols

The sulfur and nitrogen oxidation ratios (SOR and NOR) are generally used to infer the degree of atmospheric secondary transformation of SO_2 and NO_2 to sulfate and nitrate (Sahu et al., 2009; Park et al., 2013; Zhao et al., 2013). SOR and NOR values higher than 0.1 indicate secondary generation of sulfate and nitrate (Ohta and Okita, 1990; Seo et al., 2017). SOR and NOR were calculated based on the following formulas:

$$SOR = [SO_4^{2-}] / ([SO_4^{2-}] + [SO_2])$$

$$NOR = [NO_3^{-}] / ([NO_3^{-}] + [NO_2])$$

Where $[SO_4^{2-}]$ and $[NO_3^{-}]$ are the molar concentrations (μmol m^{-3}) in $PM_{2.5}$ and $[SO_2]$ and $[NO_2]$ are the molar concentrations (μmol m^{-3}) in gas phase.

3. Results

3.1 Gas concentration and meteorology for variations in $PM_{2.5}$ concentration

To identify the characteristics of high-$PM_{2.5}$ episodes, A total of 210 high-$PM_{2.5}$ episodes were analyzed during the cold season (November through March) for 2007-2019 in Seoul. Among 210 high-$PM_{2.5}$ episodes, 91 episodes (43%) lasted one day, and 119 episodes (57%) lasted more than two days. The daily average $PM_{2.5}$ concentration in high-$PM_{2.5}$ episodes exceeds 46.8 $\mu g\ m^{-3}$, almost twice the 24-h mean guideline (i.e., 25 $\mu g\ m^{-3}$) specified by the World Health Organization (WHO).

Fig. 1 illustrates the time series of the frequency of high-$PM_{2.5}$ episodes during the cold season (November-March) from 2007 to 2019 in a bar graph. In general, high-$PM_{2.5}$ episodes occurred 15 to 20 times per year, except in 2009 and 2011. The number of high-$PM_{2.5}$ episodes has remained over the past few years. Furthermore, the annual $PM_{2.5}$ concentrations in Seoul have steadily improved during 2001-2012 (Lee et al., 2018). However, the long-term decreasing trends in the concentration of $PM_{2.5}$ have weakened since 2013 (Kim et al., 2020). To establish effective mitigation plans to

reduce $PM_{2.5}$, a deep understanding of the aerosol formation, as well as verification of emission sources, is required.

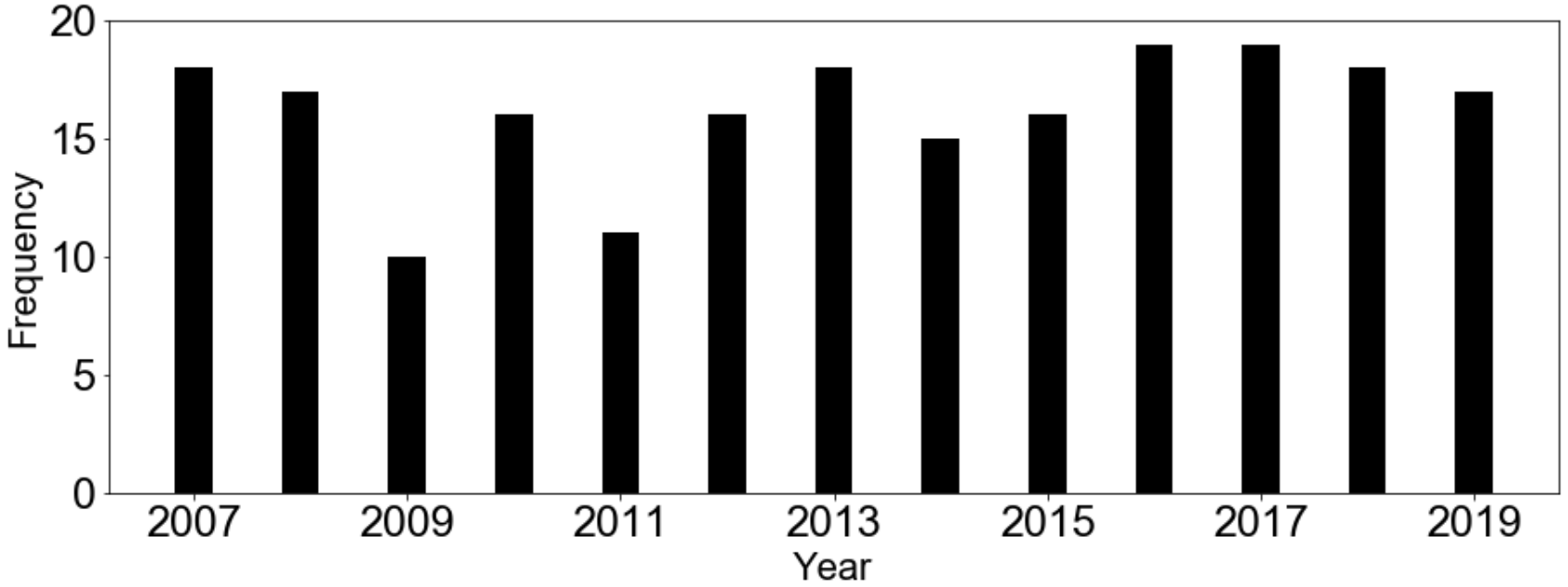

Figure 1. The number of high-$PM_{2.5}$ episodes (> 35 μ g m^{-3} day^{-1}) during the cold season (November through March) from 2007 to 2019.

3.1.1 Meteorological conditions

To identify environmental conditions associated with high−$PM_{2.5}$ episodes, meteorological variables were examined during the analysis periods in Seoul (Table 1). In the high−$PM_{2.5}$ episodes, Seoul was in relatively warmer (3.6℃), wetter (60.7%), and weaker wind (2.2 m s^{-1}) conditions compared to that in low−$PM_{2.5}$ episodes. Weak lower tropospheric winds not only prevent the dispersion of air pollutants but also allow the accumulation of particulate matter (Chaloulakou et al., 2003). Higher temperatures may be related to greater local aerosol formation because of higher rates of chemical reactions (Van Der Wal and Janssen, 2000). Furthermore, the relative humidity and total cloud cover were high during high−$PM_{2.5}$ episodes. Under these conditions, surface solar radiation does not reach the ground well, which prevents photochemical reactions. Meanwhile, many previous studies reported that high relative humidity could accumulate the aerosols by aqueous−phase reactions in cloud droplets or particles (Ravishankara et al., 1997; Zheng et al., 2015).

To understand the synoptic−scale circulations during high−$PM_{2.5}$ episodes, geopotential height, relative humidity, and temperature were analyzed for day −2 to day +2 of high−$PM_{2.5}$ episodes (Fig. 2,

3, and 4). Fig. 2 illustrates the horizontal distribution of the geopotential height anomalies at 1000, 850, and 500hPa levels. Overall, the Korean Peninsula is located at the rim of a high-pressure anomaly, whose center is near Japan from day -2 to day 0. High-$PM_{2.5}$ episodes are typically associated with anti-cyclonic circulation over the Korean Peninsula (Lee et al., 2011; Oh et al., 2015). High-pressure systems weaken airflow in the upper and lower troposphere, which is beneficial for the accumulation of air pollutants. However, high-$PM_{2.5}$ episodes are accompanied by a wide strong cyclonic circulation over northeastern of China and Mongolia. Consequently, low-pressure anomalies are dominant at the 850–1000hPa levels throughout day 0 to day +2.

Fig. 3 and 4 show horizontal distributions of the relative humidity and temperature anomalies at 1000 and 850 hPa to understand the characteristics of the synoptic-scale circulations. There were significant positive temperature anomalies at 850 hPa over the northeastern of China-Korea region from day -1 and day 0. At the same time, anomalously high relative humidity at 1000 hPa appeared in the same region. The cyclonic circulation moving eastward along with the anticyclone circulation may have introduced a warm-wet air stream into the Korean Peninsula (Fig. 2). In these meteorological

conditions, secondary aerosol formation via gas-phase and aqueous-phase reactions can be activated in the lower troposphere. However, the characteristics of meteorological fields have been analyzed based on geopotential height and wind to verify the diffusion and regional transport of air pollutants. Therefore, it is important to identify the role of meteorological fields such as high relative humidity and temperature associated with aerosol formation.

Table 1. The mean and standard deviation of meteorological variables in Seoul for all-day, high- and low-$PM_{2.5}$ episodes during cold seasons (November–March) of 2012–2018. All values are statistical significant in 99% confidence levels based on a *t*-test.

Variables	Mean ± Standard deviation		
	All-day	High-$PM_{2.5}$ episode	Low-$PM_{2.5}$ episode
Temperature (℃)	1.9 ± 5.9	3.6 ± 4.6	-0.1 ± 6.9
Relative humidity (%)	54.5 ± 13.8	60.7 ± 9.2	50.6 ± 17.6
Wind speed (m s^{-1})	2.5 ± 0.9	2.2 ± 0.6	3.1 ± 1.1
Surface solar radiation (MJ m^{-2} day^{-1})	9.1 ± 4.4	8.0 ± 3.6	9.2 ± 4.3
Total cloud cover (%)	42 ± 32	53 ± 23	34 ± 34

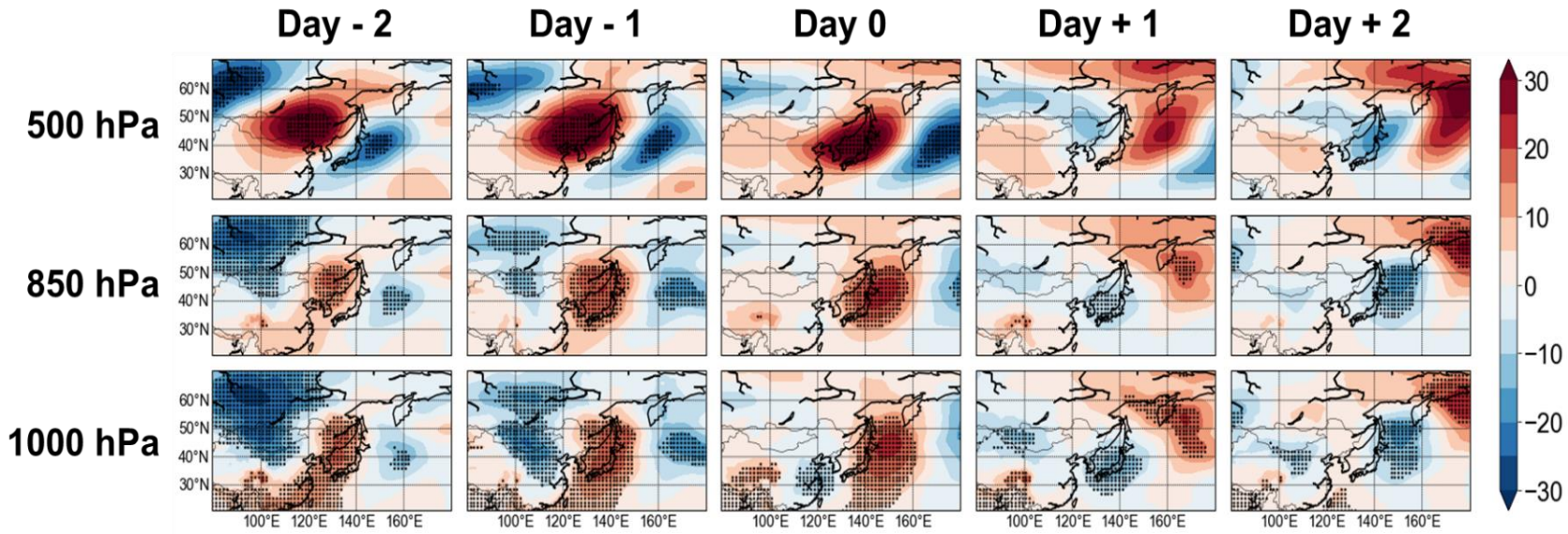

Figure 2. Composite of anomalous geopotential height at 1000-, 850-, and 500 hPa from Day -2 to Day +2 of high-$PM_{2.5}$ episodes. The anomalies were calculated against the daily climatology to remove seasonality of atmospheric fields. Black dots indicate the regions significant at the 90% confidence level.

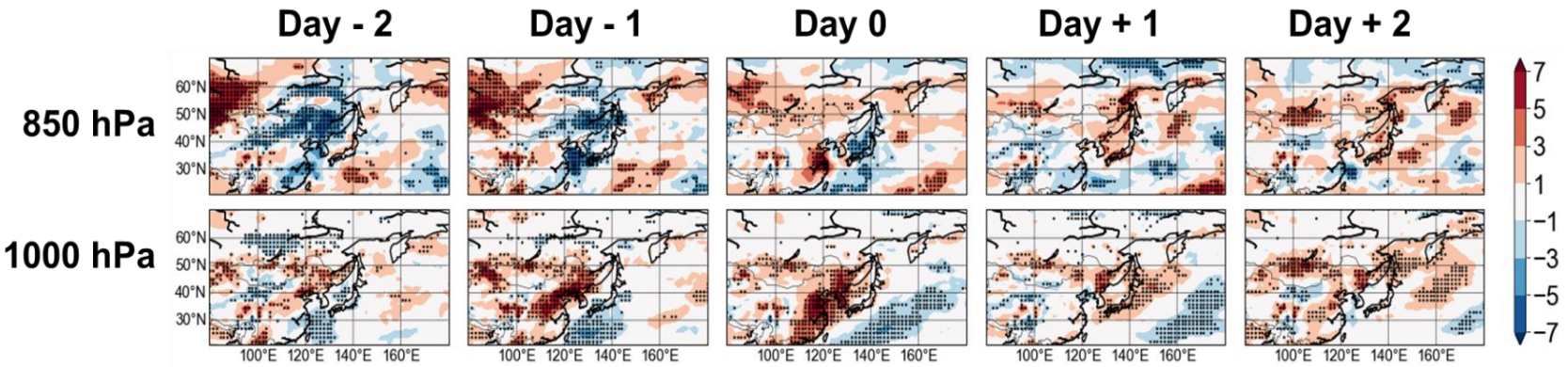

Figure 3. Composite of anomalous relative humidity at 1000-, 850-, and 500 hPa from Day -2 to Day +2 of high-$PM_{2.5}$ episodes. The anomalies were calculated against the daily climatology to remove seasonality of atmospheric fields. Black dots indicate the regions significant at the 90% confidence level.

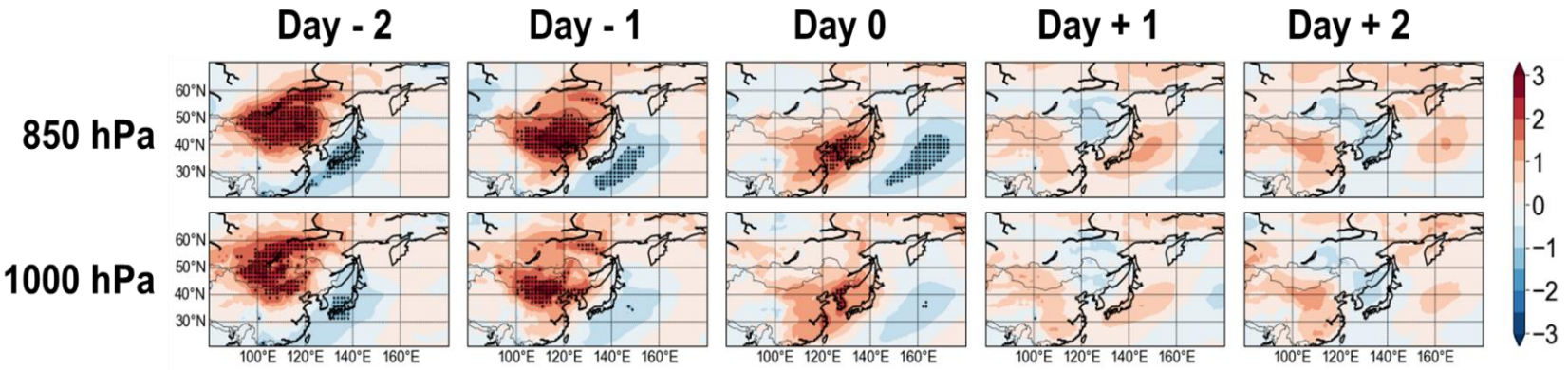

Figure 4. Composite of anomalous temperature at 1000-, 850-, and 500 hPa from Day -2 to Day +2 of high-$PM_{2.5}$ episodes. The anomalies were calculated against the daily climatology to remove seasonality of atmospheric fields. Black dots indicate the regions significant at the 90% confidence level.

3.1.2 Gaseous pollutants and major chemical components of $PM_{2.5}$

To check the chemical characteristics of high-$PM_{2.5}$ episodes, we investigated the chemical components of $PM_{2.5}$, typical gaseous pollutants, and oxidation ratios for high- and low-$PM_{2.5}$ episodes (Table 2). Since the chemical composition data of $PM_{2.5}$ is accessible from 2012 to 2018, 121 high-$PM_{2.5}$ episodes during the cold season (November through March) were analyzed. In high-$PM_{2.5}$ episodes, the daily-mean concentration of $PM_{2.5}$ exceeds 45.4 $\mu g\ m^{-3}$. Secondary inorganic aerosol (SIA) species such as sulfate (SO_4^{2-}), nitrate (NO_3^-), and ammonium (NH_4^+) accounted for 67% (30.4 $\mu g\ m^{-3}$) of the total mass of $PM_{2.5}$. However, the concentration of SIA (5.9 $\mu g\ m^{-3}$) in $PM_{2.5}$ was lower in the low-$PM_{2.5}$ episodes (11.6 $\mu g\ m^{-3}$) compared to that in the high-$PM_{2.5}$ episodes.

Many previous studies have shown that most of the SIA are generally produced through a secondary transformation in the atmosphere (Choi et al., 2019; Bae et al., 2020; Kim et al., 2020). The sulfur oxidation ratio (SOR) and nitrogen oxidation ratio (NOR) were analyzed to determine the degree of secondary formation of sulfate and nitrate (Table 2). Overall, SOR and NOR were 2.3 and 2.75 times higher in high-$PM_{2.5}$ episodes compared to that in low-

$PM_{2.5}$ episodes, respectively. In addition, the relatively high gaseous precursor and SIA compared to those in low-$PM_{2.5}$ episodes demonstrate that the conversion of gaseous precursors to particles was more active during the high-$PM_{2.5}$ episodes. The concentration of O_3 in the high-$PM_{2,5}$ episodes was lower compared to low-$PM_{2.5}$ episodes, which may be due to the relatively weak surface solar radiation and the titration of NO as air pollution persists (Seo et al., 2014).

Table 2. Same as in Table 1 except for $PM_{2.5}$ chemical compositions, typical gaseous pollutants, and oxidation ratios.

Variables	Mean ± Standard deviation		
	Average concentrations	High-$PM_{2.5}$ episode	Low-$PM_{2.5}$ episode
$PM_{2.5}$ (μ g m^{-3})	27.9 ± 14.6	45.4 ± 7.6	11.6 ± 2.4
SO_4^{2-} (μ g m^{-3})	5.0 ± 4.6	8.7 ± 4.8	2.0 ± 1.0
NO_3^- (μ g m^{-3})	8.0 ± 6.5	14.2 ± 5.9	2.5 ± 1.8
NH_4^+ (μ g m^{-3})	4.3 ± 3.3	7.6 ± 2.8	1.4 ± 0.7
SO_2 (ppb)	5.8 ± 1.9	6.9 ± 2.3	4.7 ± 1.2
NO_2 (ppb)	33.4 ± 12.4	41.8 ± 10.7	21.7 ± 6.8
O_3 (ppb)	17.0 ± 8.6	15.3 ± 9.0	20.2 ± 7.2
SOR (molar ratio)	0.16 ± 0.09	0.23 ± 0.09	0.1 ± 0.05
NOR (molar ratio)	0.07 ± 0.04	0.11 ± 0.04	0.04 ± 0.02

3.2 Influence of relative humidity on the formation of secondary inorganic aerosols in $PM_{2.5}$

To identify meteorological factors associated with secondary inorganic aerosol formation, correlations between oxidation ratios and meteorological parameters were examined during high-$PM_{2.5}$ episodes. Both SOR and NOR show a higher correlation with temperature and relative humidity among meteorological variables (Table 3). SOR shows a significant positive correlation with temperature ($r = 0.33$) and relative humidity ($r = 0.39$) during the high-$PM_{2.5}$ episodes. This result indicates that the conversion of sulfate from SO_2 can be activated through a gas or aqueous-phase reaction in a warm and wet air condition. As illustrated in the previous section, the concentrations of NO_2 and nitrate profiles were relatively higher than the other chemical constituents of $PM_{2.5}$ during the high-$PM_{2.5}$ episodes in Seoul. The high dependence of NOR on relative humidity ($r = 0.26$) reflects the role of the aqueous-phase reaction in the formation of nitrate. However, nitrate also shows a significant positive correlation ($r = 0.38$) between temperature and NOR. Nitrates are better formed at cool temperatures due to their decomposition at high temperatures, so this will be discussed later. Surface solar radiation produces oxidants through photochemical

reactions, playing a major role in gas–phase reactions together with temperature. However, surface solar radiation showed a weak positive correlation with oxidation ratios. Under high relative humidity conditions, surface solar radiation can be reduced because aerosol particles scatter more light after undergoing enhanced hygroscopic growth and aqueous–phase reaction (Tie et al., 2017).

We also analyzed variations of SOR and NOR in the range of relative humidity, surface solar radiation, and temperature to confirm the effect of the meteorological factors on the formation of sulfate and nitrate (Fig. 5). There were apparent differences in the variations in SOR and NOR under different relative humidity and temperature conditions. SOR showed no significant changes with temperature and surface solar radiation. However, SOR increased significantly with relative humidity, suggesting that the aqueous–phase reaction can make a significant contribution to the formation of sulfates (Quan et al., 2015; Zhao et al., 2013). In contrast, NOR increases with both temperature and relative humidity, suggesting the combined effects of gas– and aqueous–phase reactions. However, the NOR decreased gradually under very high temperatures (> 7 ° C) and relative humidity (> 75%). Volatilization of NH_4NO_3 at high temperatures can be a primary cause of this

phenomenon. In addition, the aqueous-phase reaction of NO_2 depends on relative humidity due to water competition for reactive surface sites of particles (Ponczek et al., 2019). Thus, the slow reduction of NOR may be due to aqueous-phase reaction suppressed under high relative humidity conditions (Tang et al., 2017). Similar to the results of correlation analysis, SOR and NOR did not show distinct variations according to surface solar radiation. However, since the effects of several meteorological factors may overlap on the production of secondary aerosol, it is necessary to separate the hidden roles of each meteorological factor.

To guess the individual effects of temperature, relative humidity, and surface solar radiation on the generation of SIA, we analyzed the correlation between oxidation ratios and meteorological parameters for each relative humidity interval (Fig. 6). Overall, the correlation of two oxidation ratios with temperature and surface solar radiation decreased with increasing relative humidity. Particularly, there is an evident nonlinear relationship in which the correlation rapidly decreased under the RH $\geq$ 60% condition. In contrast, the correlation of two oxidation ratios with relative humidity remained constant regardless of the increase in temperature and surface solar radiation (Fig. 7 and 8). These results suggest that relative humidity

always plays an important role in the formation of sulfate and nitrate. In recent previous studies, the question of what RH values convert solid particles into liquid particles remains an open debate. For example, Liu et al. and Yang et al. found that aqueous-phase reactions were activated at relatively high atmospheric RH levels (RH > 60 %) (Liu et al., 2020; Yang et al., 2020). Tian et al. proposed that the rising trend of SOR was more evident than that of NOR, especially when the RH was greater than 60% (Tian et al., 2020).

Table 3. Correlation coefficients between oxidation ratios and meteorological factors for high-$PM_{2.5}$ episodes.

	Temperature (℃)	Relative humidity (%)	Surface solar radiation (MJ m^{-2} day^{-1})
SOR	0.33*	0.39*	0.10
NOR	0.38*	0.26*	0.13

* indicates significant value at the 99% confidence level.

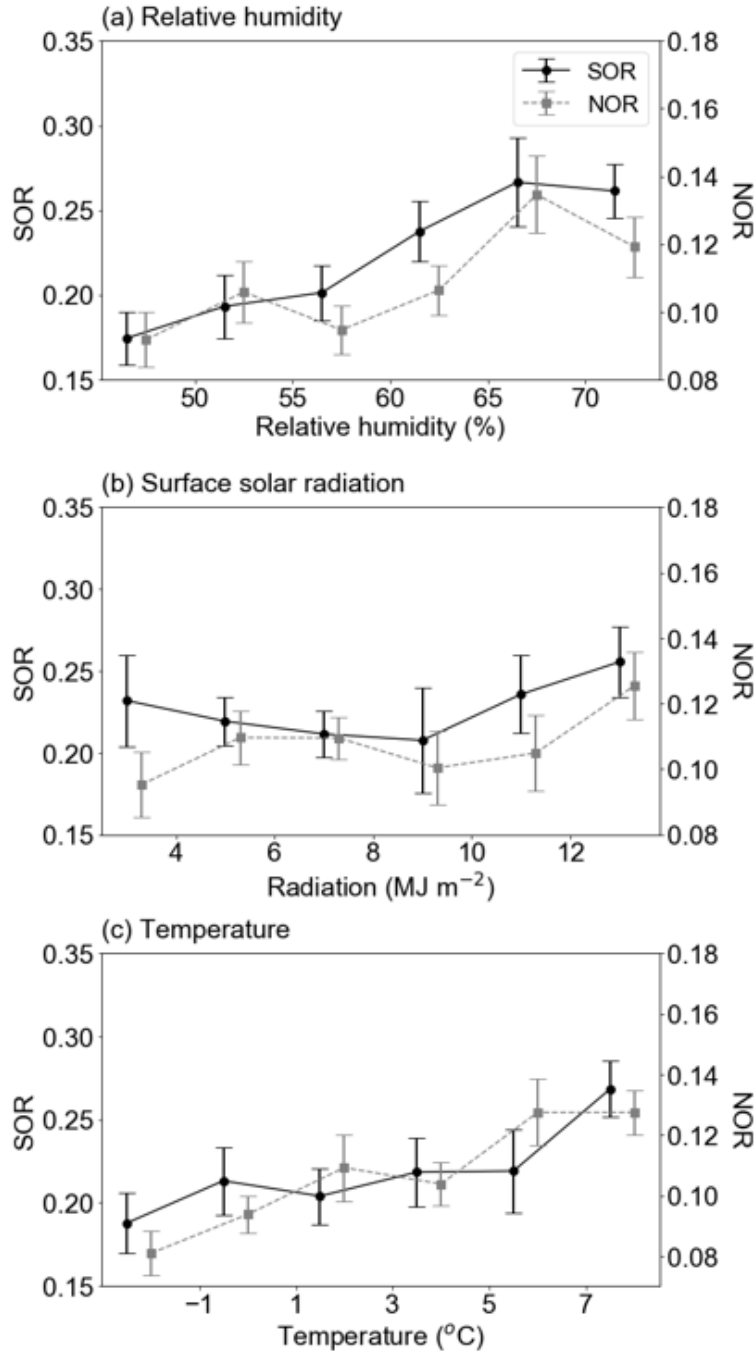

Figure 5. Relationship between oxidation ratios and meteorological variables, (a) relative humidity, (b) surface solar radiation, and (c) temperature for high-$PM_{2.5}$ episodes. The mean values are shown with standard errors.

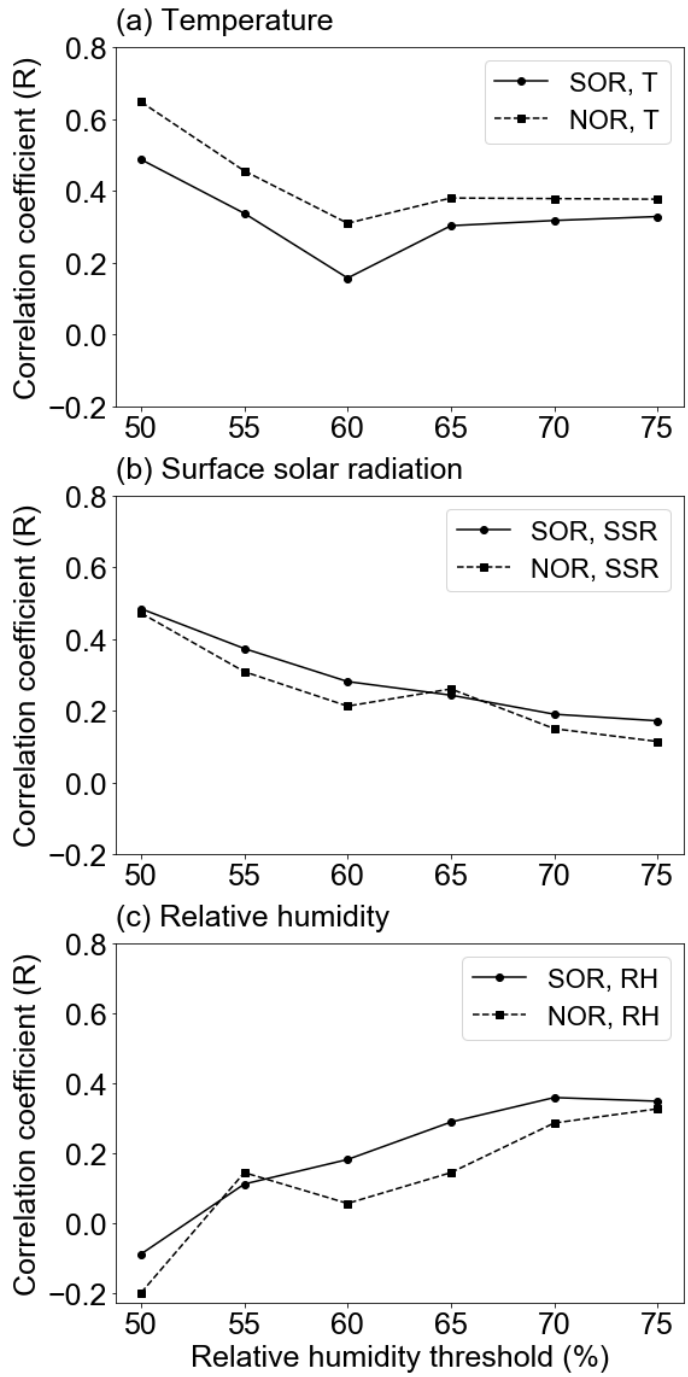

Figure 6. Correlation coefficients between oxidation ratios and meteorological variables in specified relative humidity values, (a) temperature, (b) surface solar radiation, and (c) relative humidity.

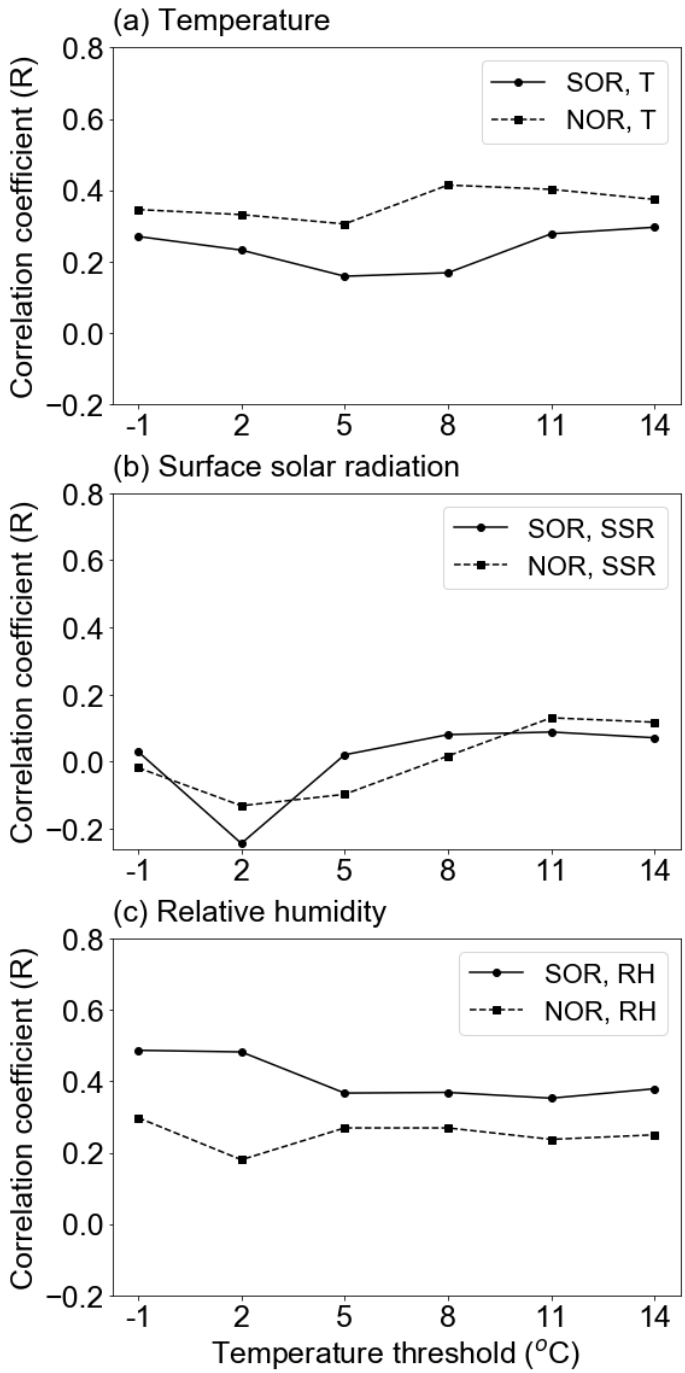

Figure 7. Correlation coefficients between oxidation ratios and meteorological variables in specified temperature values, (a) temperature, (b) surface solar radiation, and (c) relative humidity.

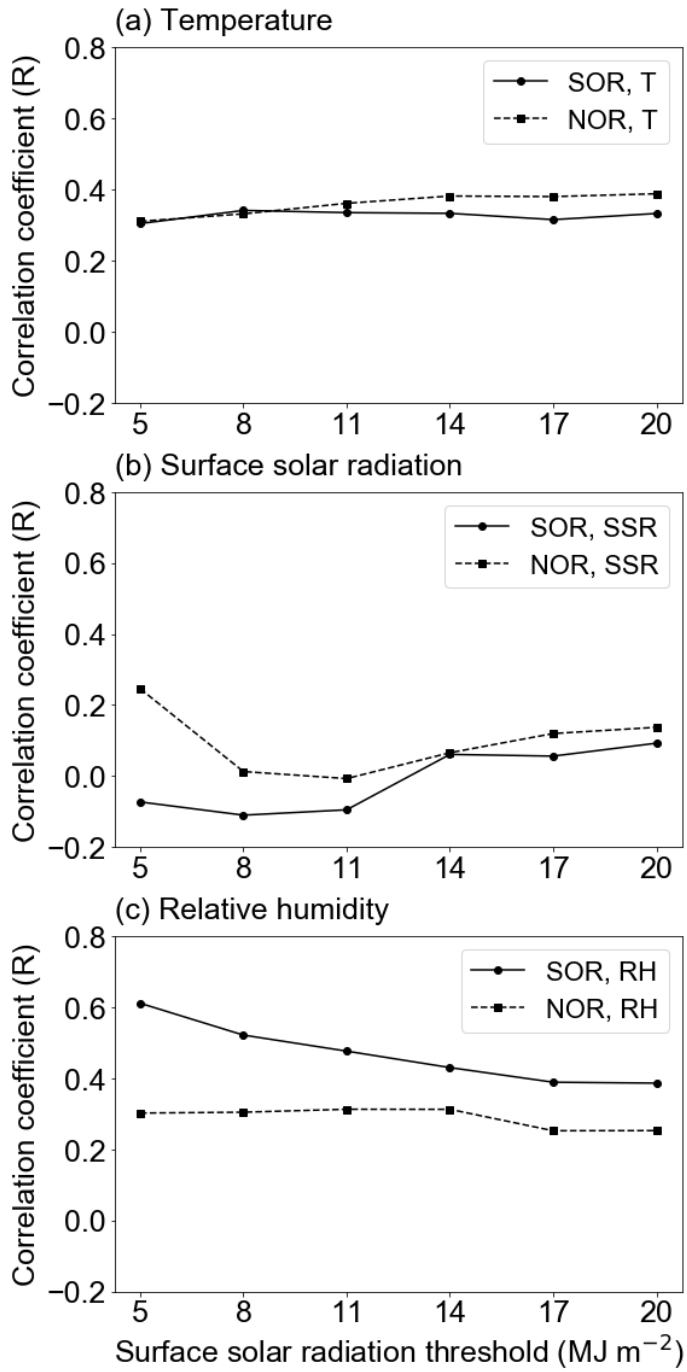

Figure 8. Correlation coefficients between oxidation ratios and meteorological variables in specified surface solar radiation values, (a) temperature, (b) surface solar radiation, and (c) relative humidity.

3.3 High-$PM_{2.5}$ episodes in wet and dry conditions

3.3.1 Chemical characteristics

We have confirmed that the meteorological factors related to the formation of SIA can change with increasing relative humidity. To check the characteristics of high-$PM_{2.5}$ episodes according to the relative humidity change, high-$PM_{2.5}$ episodes were classified into wet (RH $\geq$ 60%) and dry (RH < 60%) cases based on the threshold of relative humidity of 60%. Wet and dry cases occurred 56% (117 episodes) and 44% (93 episodes) of total cases, respectively during the cold season from 2007 to 2019.

Fig. 9 illustrates the daily-mean concentrations of $PM_{2.5}$, gaseous precursors, secondary inorganic aerosols, and oxidation ratios from day -2 to day +2 of high-$PM_{2.5}$ episodes in the wet and dry cases. In both wet and dry cases, the values of all variables began to increase from day -2 and decreased after recording the highest value on day 0. The concentration of $PM_{2.5}$ was 45 $\mu g\ m^{-3}$ in both wet and dry cases. However, the proportion of SIA to $PM_{2.5}$ was 73% (33 $\mu g\ m^{-3}$) and 62% (28 $\mu g\ m^{-3}$) in the wet and dry cases, respectively. Interestingly, the concentrations of SO_2 and NO_2 were relatively higher in dry cases than in wet cases. These results imply that the production of secondary inorganic aerosols could progress

more effectively in high relative humidity conditions.

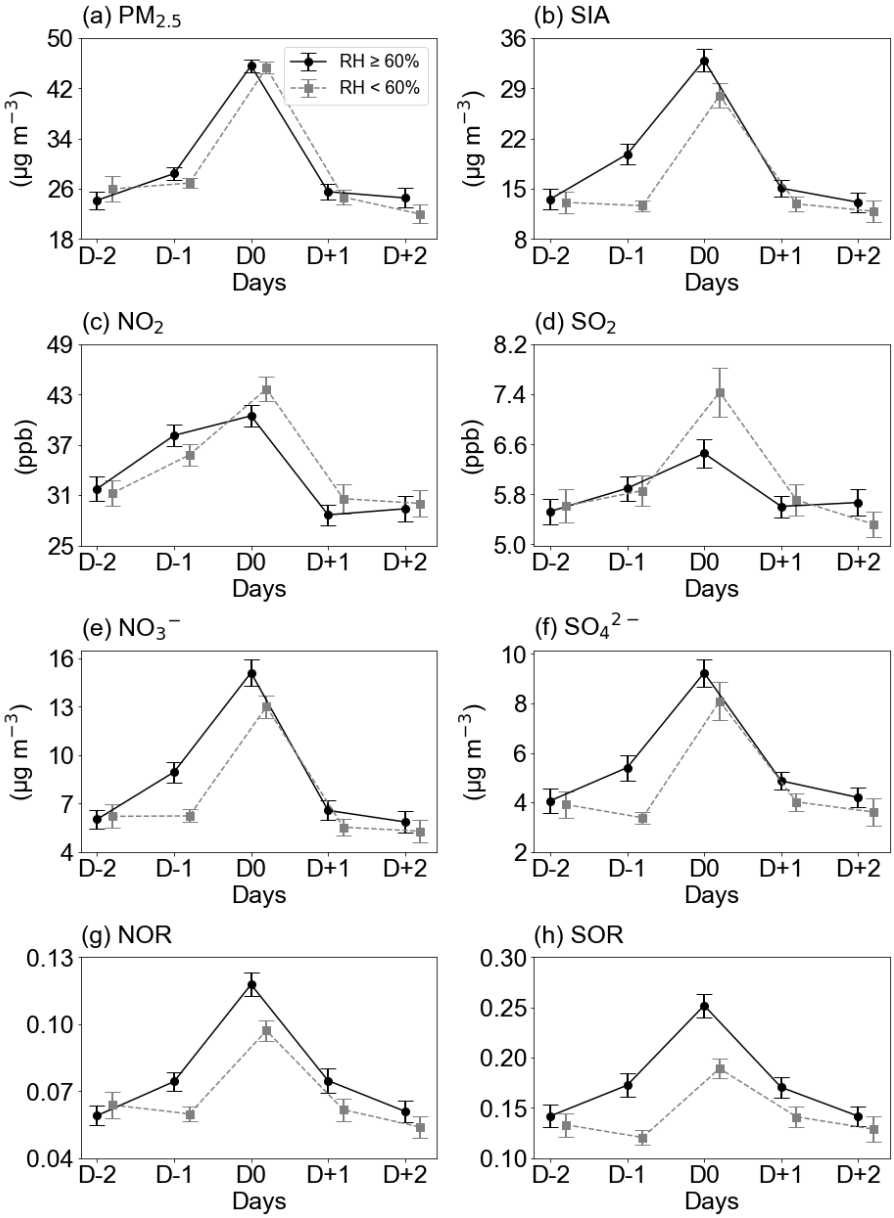

Figure 9. The daily-mean concentrations of (a) $PM_{2.5}$, (b) SIA, (c) NO_2, (d) SO_2, (e) NO_3^-, (f) SO_4^{2-}, and oxidation ratios of (g) NOR and (h) SOR for the period from Day −2 to Day +2 of high-$PM_{2.5}$ episodes under wet condition (RH ≥ 60%) and dry condition (RH < 60%).

3.3.2 Meteorological conditions

To identify meteorological conditions in wet and dry cases, we analyzed meteorological variables from day −2 to day +2 of high−$PM_{2.5}$ episodes under wet (RH ≥ 60%) and dry (RH < 60%) conditions (Fig. 10). Overall, the relative humidity was higher in the wet case than in the dry case, while the temperature was similar in both cases. In the wet cases, the relative humidity and total cloud cover increased, resulting in the decrease of the cloud bottom height from day −2 to day 0. High relative humidity and total cloud cover are favorable conditions for the activation of aqueous−phase reactions on the surface of pollutants or in−cloud processes (Ravishankara, 1997; Yang et al., 2015; Liu et al., 2020). Meanwhile, the atmospheric pressure and surface solar radiation were relatively higher in the dry cases than in the wet cases from day −2 to day 0. These results suggest that more solar radiations can be introduced into the surface, increasing the production of oxidants used in gas−phase reactions.

To understand the synoptic−scale circulations associated with high−$PM_{2.5}$ episodes in wet and dry cases, the horizontal distribution of geopotential height and relative humidity anomalies were analyzed during the analysis period (Fig. 11 and 12). In both wet and dry cases,

the Korean Peninsula was strongly affected by the high-pressure anomaly at 500 hPa levels from day -2 to day 0 (Fig. 11). However, the movement of pressure systems and the atmospheric pressure conditions in the lower troposphere were different in wet and dry cases. For the wet cases, high-$PM_{2.5}$ episodes accompanied by a wide cyclonic circulation over the northeastern of China and Mongolia from day -2. These cyclonic circulations have the property of moving eastward slowly with the anti-cyclonic circulations. Thus, low-pressure anomalies are dominant at the 850-1000 hPa levels at day 0. On the other hand, in the dry cases, strong anti-cyclonic circulation was located on the Korean Peninsula at the 500–1000 hPa on the day of high-$PM_{2.5}$ episodes. This anti-cyclonic circulation stagnated over the Korean Peninsula from day -2 to day 0.

Fig. 12 depicts the horizontal distribution of relative humidity anomalies at 1000 and 850 hPa in wet and dry cases. There were significant positive relative humidity anomalies at 1000 hPa over the eastern of China-Korea region in the wet cases from day -2 to day 0. The low-pressure anomalies caused by the cyclonic circulation may have introduced a wet air stream into the Korean Peninsula. Consequently, these meteorological conditions can provide favorable conditions for secondary aerosol formations, mainly through

aqueous-phase reactions in the lower troposphere. In contrast, negative relative humidity anomalies were significant in the dry cases at 850-1000 hPa levels throughout the entire period on the Korean Peninsula. The stagnant anti-cyclonic circulation over the Korean Peninsula may have formed dry conditions in the lower troposphere. These atmospheric conditions reach a large amount of solar radiation to the ground level, causing photochemical reactions to occur actively.

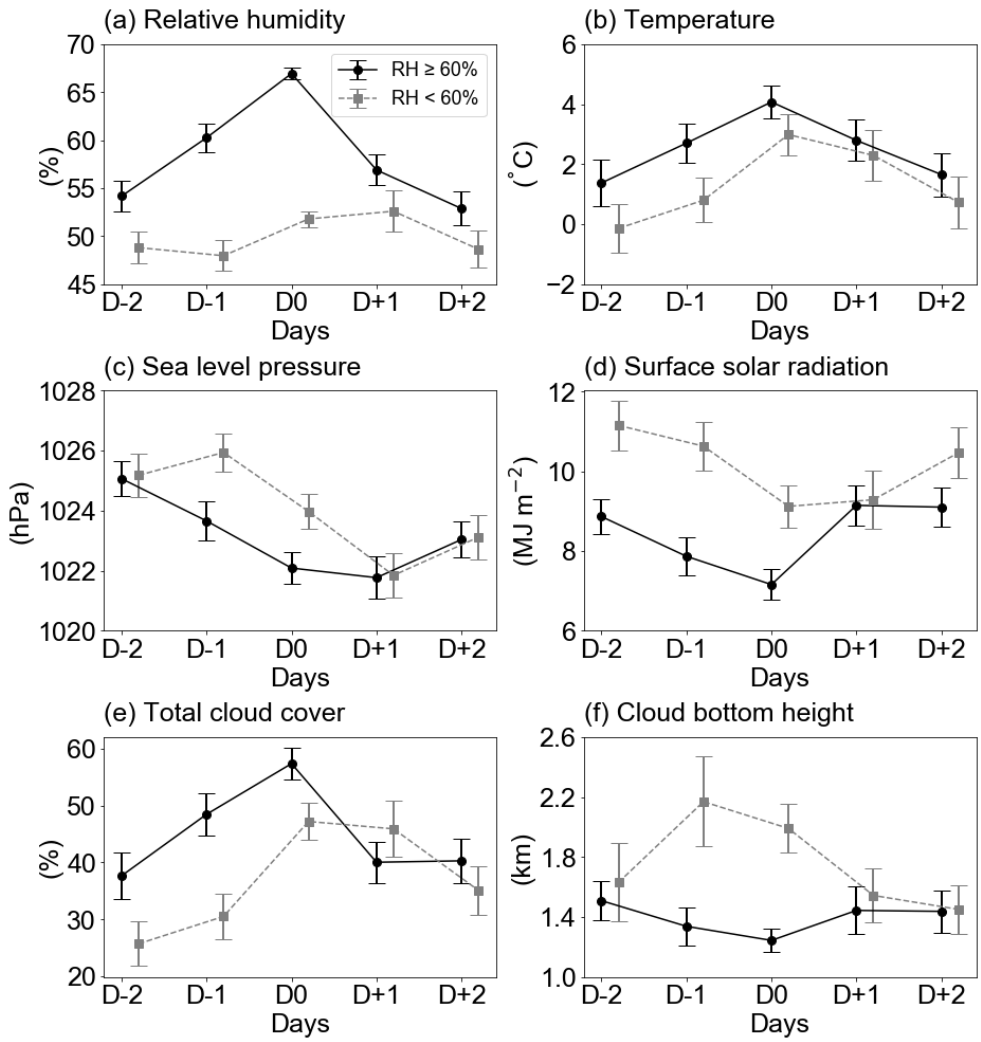

Figure 10. The daily-mean (a) relative humidity, (b) temperature, (c) sea level pressure, (d) surface solar radiation, (e) total cloud cover, and (f) cloud bottom height for the period from Day −2 to Day +2 of high-$PM_{2.5}$ episodes for the wet condition and the dry condition.

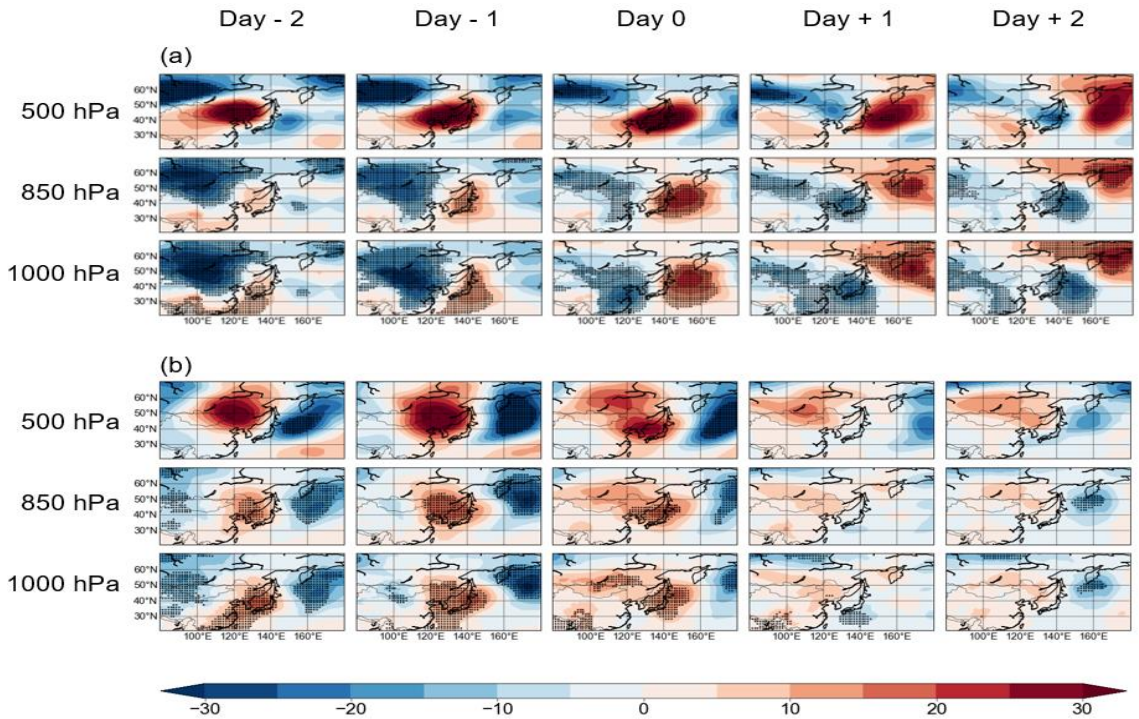

Figure 11. Composite of anomalous geopotential height at 1000-, 850-, and 500 hPa for high-$PM_{2.5}$ episodes under (a) wet and (b) dry conditions from Day −2 to Day +2 of high-$PM_{2.5}$ episodes. The anomalies were calculated against the daily climatology to remove seasonality of atmospheric fields. Black dots indicate the regions significant at the 90% confidence level.

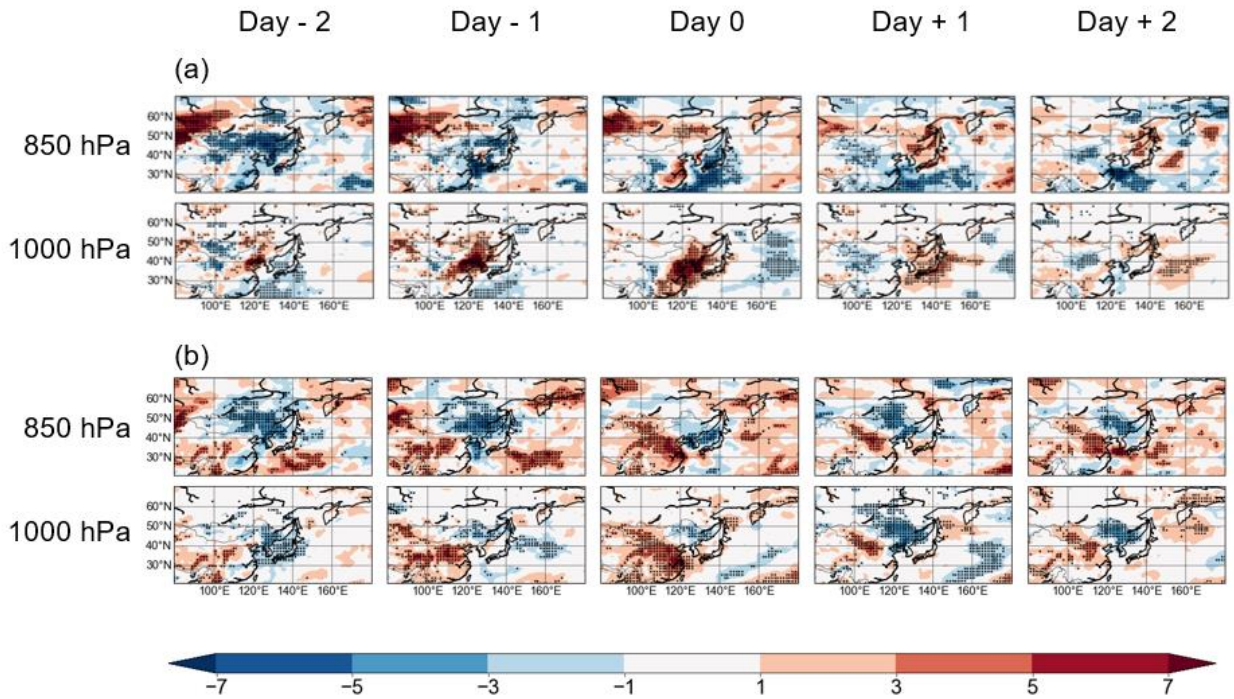

Figure 12. Composite of anomalous relative humidity at 1000-, 850-, and 500 hPa for high-$PM_{2.5}$ episodes under (a) wet and (b) dry conditions from Day −2 to Day +2 of high-$PM_{2.5}$ episodes. The anomalies were calculated against the daily climatology to remove seasonality of atmospheric fields. Black dots indicate the regions significant at the 90% confidence level.

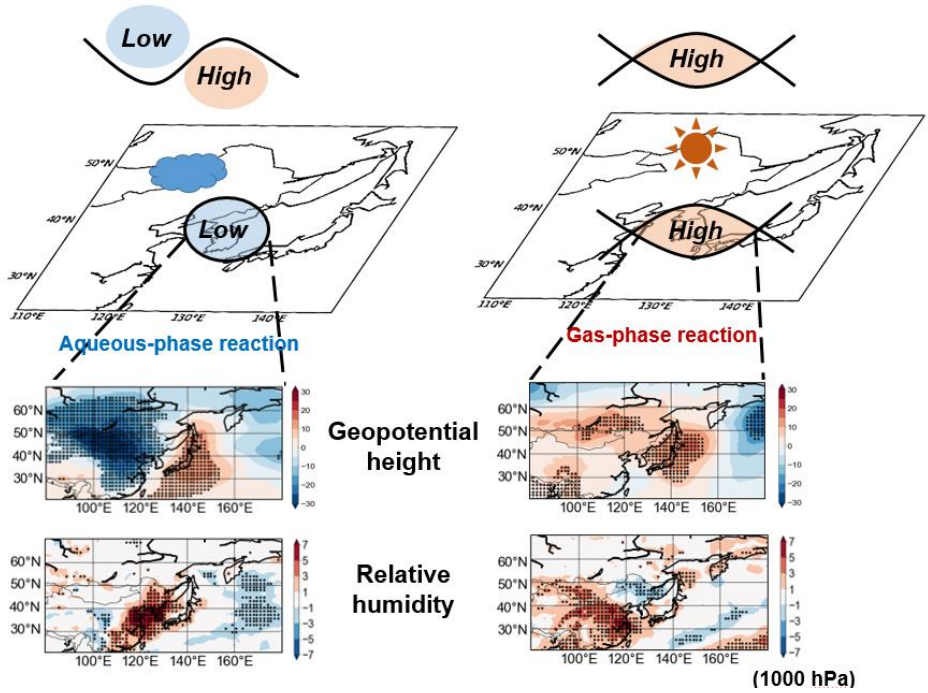

Figure 13. Schematic diagram of high-$PM_{2.5}$ episodes under the wet condition and the dry condition.

4. Concluding remarks

In this study, we identified the influence of relative humidity on high-$PM_{2.5}$ episodes during the cold season (November through March) for 2007-2019 in Seoul. Furthermore, we found that different synoptic-scale atmospheric conditions are located in the high-$PM_{2.5}$ episodes under wet (RH $\geq$ 60%) and dry (RH < 60%) conditions. The schematic diagram of the process of the studied episode is illustrated simply in Fig. 13.

During the high-$PM_{2.5}$ episodes, secondary inorganic aerosol (SIA) species such as sulfate, nitrate, and ammonium accounted for 67% (30.4 $\mu g\ m^{-3}$) of the total mass of $PM_{2.5}$. The sulfur oxidation ratio (SOR) and nitrogen oxidation ratio (NOR), which indicate the magnitude of secondary particle formation of sulfate and nitrate, increased significantly as the relative humidity increased. In particular, the relationships between the two ratios and relative humidity rapidly increased under the condition of relative humidity higher than 60%. These results suggest that the aqueous-phase reaction associated with moisture can accelerate the secondary particle formation, resulting in high-$PM_{2.5}$ episodes.

For identifying the characteristics of high-$PM_{2.5}$ episodes according to the relative humidity change, high-$PM_{2.5}$ episodes were

classified into wet (RH ≥ 60%) and dry (RH < 60%) cases based on the threshold of relative humidity of 60%. About half of the total high-$PM_{2.5}$ episodes occurred under wet conditions (RH ≥ 60%), with a higher oxidation ratios and a higher proportion of SIA than in dry conditions (RH < 60%). Composite analysis shows that low-pressure system was located in the lower troposphere due to the influence of westward-tilted trough in wet conditions from before the high-$PM_{2.5}$ episodes, resulting in high relative humidity and high total cloud cover conditions. Meanwhile, in dry condition, the stagnant high pressure was located over the Korean peninsula for a long time, which could activate the secondary formation of $PM_{2.5}$ by creating high surface solar radiation and temperature conditions. We expect that our findings will contribute to the establishing of a control policy for air pollution and assist in the forecast of air pollution episodes.

References

Adams, P. J., Seinfeld, J. H., & Koch, D. M. (1999). Global concentrations of tropospheric sulfate, nitrate, and ammonium aerosol simulated in a general circulation model. Journal of Geophysical Research Atmospheres, 104(D11), 13791–13823. https://doi.org/10.1029/1999JD900083

Alexander, B., Hastings, M. G., Allman, D. J., Dachs, J., Thornton, J. A., & Kunasek, S. A. (2009). Atmospheric Chemistry and Physics Quantifying atmospheric nitrate formation pathways based on a global model of the oxygen isotopic composition ($\triangle^{17}O$) of atmospheric nitrate. In Atmos. Chem. Phys (Vol. 9). www.atmos–chem–phys.net/9/5043/2009/

Bae, C., Kim, B. U., Kim, H. C., Yoo, C., & Kim, S. (2020). Long–range transport influence on key chemical components of $PM_{2.5}$ in the Seoul metropolitan area, south Korea, during the years 2012–2016. Atmosphere, 11(1). https://doi.org/10.3390/ATMOS11010048

Chaloulakou, A., Kassomenos, P., Spyrellis, N., Demokritou, P., & Koutrakis, P. (2003). Measurements of PM_{10} and $PM_{2.5}$ particle concentrations in Athens, Greece. Atmospheric Environment, 37(5), 649–660. https://doi.org/10.1016/S1352–

2310(02)00898-1

Chang, C. T., & Tsai, C. J. (2003). A model for the relative humidity effect on the readings of the PM_{10} beta-gauge monitor. Journal of Aerosol Science, 34(12), 1685-1697. https://doi.org/10.1016/S0021-8502(03)00356-2

Choi, J., Park, R. J., Lee, H. M., Lee, S., Jo, D. S., Jeong, J. I., Henze, D. K., Woo, J. H., Ban, S. J., Lee, M. Do, Lim, C. S., Park, M. K., Shin, H. J., Cho, S., Peterson, D., & Song, C. K. (2019). Impacts of local vs. trans-boundary emissions from different sectors on $PM_{2.5}$ exposure in South Korea during the KORUS-AQ campaign. Atmospheric Environment, 203(September 2018), 196-205. https://doi.org/10.1016/j.atmosenv.2019.02.008

Ghim, Y. S., Oh, yun S., & Chang, Y. S. (2001). Meteorological effects on the evolution of high ozone episodes in the greater Seoul area. Journal of the Air and Waste Management Association, 51(2), 185-202. https://doi.org/10.1080/10473289.2001.10464269

Guo, H., Otjes, R., Schlag, P., Kiendler-Scharr, A., Nenes, A., & Weber, R. J. (2018). Effectiveness of ammonia reduction on control of fine particle nitrate. Atmospheric Chemistry and Physics, 18(16), 12241-12256. https://doi.org/10.5194/acp-18-12241-2018

Hur, S. K., Oh, H. R., Ho, C. H., Kim, J., Song, C. K., Chang, L. S., & Lee, J. B. (2016). Evaluating the predictability of PM_{10} grades in Seoul, Korea using a neural network model based on synoptic patterns. Environmental Pollution, 218, 1324–1333.

Jang, E., Do, W., Park, G., Kim, M., & Yoo, E. (2017). Spatial and temporal variation of urban air pollutants and their concentrations in relation to meteorological conditions at four sites in Busan, South Korea. Atmospheric Pollution Research, 8(1), 89–100. https://doi.org/10.1016/j.apr.2016.07.009

Jung, C.–H., Cho, Y.–S., Hwang, S. M., Jung, Y. G., Ryu, J. C., & Shin, D. S. (2007). Analysis of Measurement Error for PM–10 Mass Concentration by Inter–Comparison Study. In Journal of Korean Society for Atmospheric Environment (Vol. 23, Issue 6, pp. 689–698). https://doi.org/10.5572/kosae.2007.23.6.689

Jung, M. I., Son, S. W., Kim, H. C., Kim, S. W., Park, R. J., & Chen, D. (2019). Contrasting synoptic weather patterns between non–dust high particulate matter events and Asian dust events in Seoul, South Korea. Atmospheric Environment, 214, 116864.

Kim, H. S., Huh, J. B., Hopke, P. K., Holsen, T. M., & Yi, S. M. (2007). Characteristics of the major chemical constituents of $PM_{2.5}$ and smog events in Seoul, Korea in 2003 and 2004. Atmospheric

Environment, 41(32), 6762-6770. https://doi.org/10.1016/j.atmosenv.2007.04.060

Kim, Y., Yi, S. M., & Heo, J. (2020). Fifteen-year trends in carbon species and $PM_{2.5}$ in Seoul, South Korea (2003-2017). Chemosphere, 261, 127750. https://doi.org/10.1016/j.chemosphere.2020.127750

Lee, G., Oh, H. R., Ho, C. H., Park, D. S. R., Kim, J., Chang, L. S., Lee, J. B., Choi, J., & Sung, M. (2018). Slow decreasing tendency of fine particles compared to coarse particles associated with recent hot summers in Seoul, Korea. Aerosol and Air Quality Research, 18(9), 2185-2194. https://doi.org/10.4209/aaqr.2017.10.0403

Lee, S., Ho, C. H., & Choi, Y. S. (2011). High-PM_{10} concentration episodes in Seoul, Korea: Background sources and related meteorological conditions. Atmospheric Environment, 45(39), 7240-7247. https://doi.org/10.1016/j.atmosenv.2011.08.071

Liu, P., Ye, C., Xue, C., Zhang, C., Mu, Y., & Sun, X. (2020). Formation mechanisms of atmospheric nitrate and sulfate during the winter haze pollution periods in Beijing: Gas-phase, heterogeneous and aqueous-phase chemistry. Atmospheric Chemistry and Physics, 20(7), 4153-4165. https://doi.org/10.5194/acp-20-4153-

2020

Liu, Y., Wu, Z., Wang, Y., Xiao, Y., Gu, F., Zheng, J., Tan, T., Shang, D., Wu, Y., Zeng, L., Hu, M., Bateman, A. P., & Martin, S. T. (2017). Submicrometer Particles Are in the Liquid State during Heavy Haze Episodes in the Urban Atmosphere of Beijing, China. Environmental Science and Technology Letters, 4(10), 427-432. https://doi.org/10.1021/acs.estlett.7b00352

National Institute of Environmental Research (NIER) (2018) 2018 Intensive Air Quality Monitoring station Annual Operation Result Report, http://www.airkorea.or.kr

Ning, G., Wang, S., Yim, S. H. L., Li, J., Hu, Y., Shang, Z., Wang, J., & Wang, J. (2018). Impact of low-pressure systems on winter heavy air pollution in the northwest Sichuan Basin, China. Atmospheric Chemistry and Physics, 18(18), 13601-13615. https://doi.org/10.5194/acp-18-13601-2018

Oh, H. R., Ho, C. H., Kim, J., Chen, D., Lee, S., Choi, Y. S., Chang, L. S., & Song, C. K. (2015). Long-range transport of air pollutants originating in China: A possible major cause of multi-day high-PM_{10} episodes during cold season in Seoul, Korea. Atmospheric Environment, 109, 23-30. https://doi.org/10.1016/j.atmosenv.2015.03.005

Ohta, S., & Okita, T. (1990). A chemical characterization of atmospheric aerosol in Sapporo. Atmospheric Environment Part A, General Topics, 24(4), 815-822. https://doi.org/10.1016/0960-1686(90)90282-R

Park, E. H., Heo, J., Kim, H., & Yi, S. M. (2020). Long term trends of chemical constituents and source contributions of $PM_{2.5}$ in Seoul. Chemosphere, 251. https://doi.org/10.1016/j.chemosphere.2020.126371

Park, S. M., Moon, K. J., Park, J. S., Kim, H. J., Ahn, J. Y., & Kim, J. S. (2012). Chemical Characteristics of Ambient Aerosol during Asian Dusts and High PM Episodes at Seoul Intensive Monitoring Site in 2009. Journal of Korean Society for Atmospheric Environment, 28(3), 282-293.

Park, S. S., Jung, S. A., Gong, B. J., Cho, S. Y., & Lee, S. J. (2013). Characteristics of $PM_{2.5}$ haze episodes revealed by highly time-resolved measurements at an air pollution monitoring supersite in Korea. Aerosol and Air Quality Research, 13(3), 957-976. https://doi.org/10.4209/aaqr.2012.07.0184

Ponczek, M., Hayeck, N., Emmelin, C., & George, C. (2019). Heterogeneous photochemistry of dicarboxylic acids on mineral dust. Atmospheric Environment, 212(January), 262-271.

https://doi.org/10.1016/j.atmosenv.2019.05.032

Quan, J., Liu, Q., Li, X., Gao, Y., Jia, X., Sheng, J., & Liu, Y. (2015). Effect of heterogeneous aqueous reactions on the secondary formation of inorganic aerosols during haze events. Atmospheric Environment, 122, 306-312. https://doi.org/10.1016/j.atmosenv.2015.09.068

Ravishankara, A. R. (1997). Heterogeneous and multiphase chemistry in the troposphere. Science, 276(5315), 1058-1065. https://doi.org/10.1126/science.276.5315.1058

Sahu, L. K., Kondo, Y., Miyazaki, Y., Kuwata, M., Koike, M., Takegawa, N., Tanimoto, H., Matsueda, H., Yoon, S. C., & Kim, Y. J. (2009). Anthropogenic aerosols observed in Asian continental outflow at Jeju Island, Korea, in spring 2005. Journal of Geophysical Research Atmospheres, 114(3), 1-19. https://doi.org/10.1029/2008JD010306

Seo, J., Youn, D., Kim, J. Y., & Lee, H. (2014). Extensive spatiotemporal analyses of surface ozone and related meteorological variables in South Korea for the period 1999–2010. Atmospheric Chemistry and Physics, 14(12), 6395-6415. https://doi.org/10.5194/acp-14-6395-2014

Seo, J., Kim, J. Y., Youn, D., Lee, J. Y., Kim, H., Lim, Y. Bin, Kim, Y.,

& Cher Jin, H. (2017). On the multiday haze in the Asian continental outflow: The important role of synoptic conditions combined with regional and local sources. Atmospheric Chemistry and Physics, 17(15), 9311-9332. https://doi.org/10.5194/acp-17-9311-2017

Shin, S. E., Jung, C. H., & Kim, Y. P. (2011). Analysis of the measurement difference for the PM_{10} concentrations between beta-ray absorption and gravimetric methods at gosan. Aerosol and Air Quality Research, 11(7), 846-853. https://doi.org/10.4209/aaqr.2011.04.0041

Shu, L., Xie, M., Gao, D., Wang, T., Fang, D., Liu, Q., Huang, A., & Peng, L. (2017). Regional severe particle pollution and its association with synoptic weather patterns in the Yangtze River Delta region, China. Atmospheric Chemistry and Physics, 17(21), 12871-12891. https://doi.org/10.5194/acp-17-12871-2017

Smith, N., Plane, J. M. C., & Solomon, P. A. (1995). Atmospheric Enuironment (Vol. 29, Issue 21).

Tang, M., Huang, X., Lu, K., Ge, M., Li, Y., Cheng, P., Zhu, T., Ding, A., Zhang, Y., Gligorovski, S., Song, W., Ding, X., Bi, X., & Wang, X. (2017). Heterogeneous reactions of mineral dust aerosol: Implications for tropospheric oxidation capacity. Atmospheric

Chemistry and Physics, 17(19), 11727-11777. https://doi.org/10.5194/acp-17-11727-2017

Tian, S., Liu, Y., Wang, J., Wang, J., Hou, L., Lv, B., ... & Bai, Z. (2020). Chemical Compositions and Source Analysis of $PM_{2.5}$ during Autumn and Winter in a Heavily Polluted City in China. Atmosphere, 11(4), 336.

Tie, X., Huang, R. J., Cao, J., Zhang, Q., Cheng, Y., Su, H., ... & O'Dowd, C. D. (2017). Severe pollution in China amplified by atmospheric moisture. Scientific Reports, 7(1), 1-8.

Wai, K. M., & Tanner, P. A. (2005). Relationship between ionic composition in PM_{10} and the synoptic-scale and mesoscale weather conditions in a south China coastal city: A 4-year study. Journal of Geophysical Research D: Atmospheres, 110(18), 1-13. https://doi.org/10.1029/2004JD005385

Wang, G., Zhang, R., Gomez, M. E., Yang, L., Zamora, M. L., Hu, M., Lin, Y., Peng, J., Guo, S., Meng, J., Li, J., Cheng, C., Hu, T., Ren, Y., Wang, Y., Gao, J., Cao, J., An, Z., Zhou, W., … Molina, M. J. (2016). Persistent sulfate formation from London Fog to Chinese haze. Proceedings of the National Academy of Sciences of the United States of America, 113(48), 13630-13635. https://doi.org/10.1073/pnas.1616540113

Wang, Y., Zhuang, G., Sun, Y., & An, Z. (2006). The variation of characteristics and formation mechanisms of aerosols in dust, haze, and clear days in Beijing. Atmospheric Environment, 40(34), 6579-6591. https://doi.org/10.1016/j.atmosenv.2006.05.066

Wu, Z., Wang, Y., Tan, T., Zhu, Y., Li, M., Shang, D., Wang, H., Lu, K., Guo, S., Zeng, L., & Zhang, Y. (2018). Aerosol Liquid Water Driven by Anthropogenic Inorganic Salts: Implying Its Key Role in Haze Formation over the North China Plain. Environmental Science and Technology Letters, 5(3), 160-166. https://doi.org/10.1021/acs.estlett.8b00021

Yang, S., Duan, F., Ma, Y., Li, H., Ma, T., Zhu, L., ... & He, K. (2020). Mixed and intensive haze pollution during the transition period between autumn and winter in Beijing, China. Science of The Total Environment, 711, 134745.

Yang, Y. R., Liu, X. G., Qu, Y., An, J. L., Jiang, R., Zhang, Y. H., Sun, Y. L., Wu, Z. J., Zhang, F., Xu, W. Q., & Ma, Q. X. (2015). Characteristics and formation mechanism of continuous hazes in China: A case study during the autumn of 2014 in the North China Plain. Atmospheric Chemistry and Physics, 15(14), 8165-8178. https://doi.org/10.5194/acp-15-8165-2015

You, T., Wu, R., Huang, G., & Fan, G. (2017). Regional meteorological patterns for heavy pollution events in Beijing. Journal of Meteorological Research, 31(3), 597-611. https://doi.org/10.1007/s13351-017-6143-1

Zhao, S., Feng, T., Tie, X., Long, X., Li, G., Cao, J., Zhou, W., & An, Z. (2018). Impact of Climate Change on Siberian High and Wintertime Air Pollution in China in Past Two Decades. Earth's Future, 6(2), 118-133. https://doi.org/10.1002/2017EF000682

Zhao, X. J., Zhao, P. S., Xu, J., Meng, W., Pu, W. W., Dong, F., He, D., & Shi, Q. F. (2013). Analysis of a winter regional haze event and its formation mechanism in the North China Plain. Atmospheric Chemistry and Physics Discussions, 13(1), 903-933. https://doi.org/10.5194/acpd-13-903-2013

Zheng, G. J., Duan, F. K., Su, H., Ma, Y. L., Cheng, Y., Zheng, B., Zhang, Q., Huang, T., Kimoto, T., Chang, D., Pöschl, U., Cheng, Y. F., & He, K. B. (2015). Exploring the severe winter haze in Beijing: The impact of synoptic weather, regional transport and heterogeneous reactions. Atmospheric Chemistry and Physics, 15(6), 2969-2983. https://doi.org/10.5194/acp-15-2969-2015

국문 초록

공기역학적 직경이 2.5 μm ($PM_{2.5}$)보다 작은 입자상 물질의 고농도 에피소드는 일반적으로 온난하고 안정적인 고기압 조건에서 발생한다. 이 연구는 2007–2019년 추운 계절(11–3월) 동안 서울에서 저기압 시스템의 습한 조건이 고농도 $PM_{2.5}$ 에피소드에 중요한 역할을 함을 발견하였다. 고농도 기간 $PM_{2.5}$의 주요 화학 성분은 황산염, 질산염, 그리고 암모늄과 같은 2차 무기 에어로졸(SIA) 이었다. 황산염과 질산염의 2차 생성 정도를 나타내는 황 및 질소 산화 비율은 주로 상대습도(RH)에 따라 선형적으로 증가하였다. 특히 가스상 전구물질에서 2차 무기 에어로졸로 전환은 RH가 60%보다 높은 경우에 활성화되었다. 이러한 결과는 습기와 연관된 수상 반응이 에어로졸의 2차 생성을 가속하여 고농도 $PM_{2.5}$ 에피소드를 유발할 수 있음을 시사한다. 고농도 $PM_{2.5}$ 에피소드의 절반 이상이 상대습도 60% 이상의 조건에서 발생하였으며, 서쪽으로 편향된 기압골이 대류권 하층에 위치하였다. 반대로, 상대습도 60% 미만의 고농도 $PM_{2.5}$ 에피소드는 정체된 고기압 시스템 영향 아래 강한 일사량에 의한 광화학 반응과 관련 있었다. 이 연구는 대류권 하층에서 저기압 시스템을 동반한 높은 상대습도가 $PM_{2.5}$ 고농도 현상을 유발할 수 있으며, 대기질 예측에서 고려되어야 할 중요 기상 조건임을 시사한다.

주요어 : 초 미세먼지, 상대습도, 2차 무기 에어로졸, 수상 반응, 서울
학 번 : 2019-23307